Taylor & Francis
Taylor & Francis Group

SEPARATION SCIENCE AND TECHNOLOGY

Separation Science and Technology

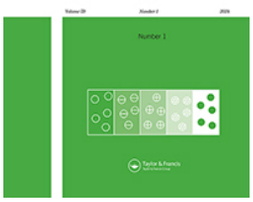

ISSN: 0149-6395 (Print) 1520-5754 (Online) Journal homepage: www.tandfonline.com/journals/lsst20

Potential of microwave-assisted hydrothermal modification for enhanced fly ash adsorption capacity toward to heavy metals: A comprehensive investigation of adsorbent characterization, isotherms, kinetics, and thermodynamics

Gamzenur Özsin & Esin Apaydin Varol

To cite this article: Gamzenur Özsin & Esin Apaydin Varol (2024) Potential of microwave-assisted hydrothermal modification for enhanced fly ash adsorption capacity toward to heavy metals: A comprehensive investigation of adsorbent characterization, isotherms, kinetics, and thermodynamics, Separation Science and Technology, 59:1, 71-86, DOI: 10.1080/01496395.2024.2315611

To link to this article: https://doi.org/10.1080/01496395.2024.2315611

SEPARATION SCIENCE AND TECHNOLOGY
2024, VOL. 59, NO. 1, 71–86
https://doi.org/10.1080/01496395.2024.2315611

Taylor & Francis
Taylor & Francis Group

Potential of microwave-assisted hydrothermal modification for enhanced fly ash adsorption capacity toward to heavy metals: A comprehensive investigation of adsorbent characterization, isotherms, kinetics, and thermodynamics

Gamzenur Özsin[a,b] and Esin Apaydin Varol[c]

[a]Faculty of Engineering, Department of Chemical Engineering, Bilecik Şeyh Edebali University, Bilecik, Turkey; [b]Imperial College London, Faculty of Engineering, Department of Chemical Engineering, London, UK; [c]Faculty of Engineering, Department of Chemical Engineering, Eskişehir Technical University, Eskisehir, Turkey

ABSTRACT

Heavy metal contamination is a major concern, and the adsorption process is regarded as one of the most efficient water remediation processes to deal with it. Herein, we modified fly ash by a microwave-assisted hydrothermal process to enhance its adsorption capacity and tested the material toward Cd(II) and Cu(II). Characterization of the adsorbents was performed by several techniques in detail to elucidate considerable structural changes such as cracking of spherical morphology, increase in surface area and changing of the chemical composition. Then batch adsorption was performed under different conditions to investigate the equilibrium, kinetics, and thermodynamics of the process. NaOH-modified fly ash considerably has a higher adsorption performance than that of the as-received sample for both ions. The highest adsorption capacity of modified fly ash was achieved as 133.8 and 95.7 mg/g for Cd(II) and Cu(II), respectively. The kinetics and isotherms could be perfectly reflected by a pseudo-second-order rate equation and the Freundlich model, while thermodynamics confirmed the endothermicity of the process.

ARTICLE HISTORY
Received 6 September 2023
Accepted 9 January 2024

KEYWORDS
Fly ash; adsorption; heavy metal; microwave modification; isotherm; kinetics and thermodynamics

Introduction

The rapid industrialization and human activities associated with socioeconomic growth have raised serious concerns about the toxicity of non-biodegradable heavy metals. These metals persist in water, pose threats to human health, and accumulate in the food chain.[1,2] Therefore, heavy metal removal technologies have drawn considerable attention in the last decades.[3] To mitigate the harmful effects of heavy metals on the aquatic environment, it is essential to reduce the concentration originating from industrial facilities. For instance, divalent cadmium [Cd(II)] and copper [Cu(II)] are broadly used in industrial sectors including the production of batteries, pigments, fertilizers, metals, and alloys. These heavy metals must be released to wastewaters with the permissible levels of 0.005 mg/L and 1.3 mg/L, respectively, according to the United States Environmental Protection Agency (EPA).[4] Therefore, various treatment techniques including adsorption, precipitation, membrane filtration, chemical oxidation, and ion exchange have been used to date to manage the heavy metal contamination of industrial effluent.[5–7] However, most procedures are exorbitant, time-consuming, and problematic in terms of waste disposal.[8,9] Among the wastewater treatment methods, the adsorption process is easy to handle, economically advantageous, and most effective when adopting an adsorbent with a high capacity for the target pollutant removal process.[10,11] Another significant benefit of this method is the ability to create and use designed materials with specific properties for improved adsorption performance.[12,13]

The capacity of the adsorbent to adsorb is the foremost factor determining the effectiveness of the adsorbent and, consequently, the viability of the adsorption processes. Several adsorbents with high adsorption capacity have been proven to have good performance toward heavy metals up to date.[14–16] Natural and synthetic adsorbents such as activated carbon, biosorbents, clays, polymer-based adsorbents, resins, and nanoparticles have specific surface properties and functional groups that make them effective at heavy metal adsorption. They are known to contribute to the heavy metal removal processes via mechanisms that may include ion exchange, physisorption, chemisorption, complexation, chelation, and precipitation. However, many of the reported sorbent materials might have limited efficiency, selectivity, reusability, or poor stability in

CONTACT Gamzenur Özsin gozsin@anadolu.edu.tr Faculty of Engineering, Bilecik Şeyh Edebali University, Department of Chemical Engineering, Bilecik 11210, Turkey

aqueous media with high synthesis and operation costs and hence they have a limited practical applicability.[17] Therefore, some strategies are provided for modification of adsorbents is gradually emerging to develop low-cost adsorbent materials with a high adsorption capacity.[18,19] To enhance adsorption capacity, modification is a common technique that involves changing the surface properties of the adsorbent. Chemical modification primarily focuses on introducing or enhancing functional groups capable of interacting with heavy metals and modifying surface charges.[20–22] On the other hand, physical modification involves changing the physical properties of the adsorbent material, such as its particle size or pore size, to increase its capacity for heavy metal ion removal.[23] It is beneficial that certain techniques can combine the advantages of both physical and chemical modification, thereby altering both the physical properties and chemical structure of sorbent materials.

As a by-product of burning pulverized coal in thermal power plants, powdered fly ash has been proven to be effective in the adsorption of heavy metal ions as it can be concluded from previous studies.[24–28] Massive amounts of waste fly ash generation in coal-based power plants with a global annual production exceeding 600 million tonnes will also serve as an advantage in terms of cost reduction for selective adsorbent production toward heavy metals if they can be managed properly.[29–31] However, there is a still gap in the enhancement of limited adsorptive capacity of the fly ash to the best of our knowledge despite several studies worked on evaluating different kinds of ashes from different coal combustion residues.[32–34] The determination of effects of surface modification techniques, altering morphology (the porosity and surface area), optimization of the adsorption conditions, scaling-up, and evaluating environmental impact to meet the requirements of the regulatory compliances in research can enhance the performance of fly ash as an adsorbent in real industrial heavy metal removal processes. In this study, efforts had been devoted to the modify FA that can maintain good adsorption capacity in heavy metal containing aqueous solutions. To enhance the adsorption ability to different types of heavy metals, microwave-assisted alkali hydrothermal process was applied, and the products were characterized in detail. This procedure was designed to achieve improved adsorbent quality with higher adsorption capacities since microwave-assisted alkali hydrothermal treatment enables to synthesis of functional materials with a faster process and energy efficiency by applying selective and uniform heating combined with alkali treatment.[35,36] After modification process, adsorption behavior of modified and unmodified material, and the effects of process conditions such as adsorbent dose, temperature, contact time, and initial adsorbate concentration were investigated. The detailed studies of adsorption isotherms, kinetics, and thermodynamics, as well as comprehensive characterization studies aimed to establish more effective management strategies for adsorptive heavy metal removal using a low-cost industrial waste.

Materials and methods

Determination of the main characteristics of fly ash

The fly ash sample was obtained from a local cement plant located in Bilecik, Turkey. The sample was produced through the bituminous coal combustion unit of the cement plant and collected from electrostatic precipitators. Moreover, it is also known to be used as a supplementary cementitious material, replacing a portion of the clinker in the plant. Prior to its use in the experiments, the sample was dried at 80°C. Afterward, the characteristics of the sample were determined using several analytical methods. The same analytical tools were used to investigate the characteristics of FA before and after modification to describe the surface structure of the material and interpret the adsorption mechanism. The surface morphology and microstructure of the samples were analyzed by scanning electron microscope (Carl Zeiss Supra 40VP) using secondary electron images. The specific surface area of the samples was assessed using a pore-size analyzer (Quantachrome Autosorb) through multi-point N_2 adsorption/desorption. All samples were degassed at 150°C for 12 hours prior to N_2 adsorption and surface area values were obtained by using the Brunauer–Emmett–Teller (BET) equation from the isotherms obtained at 196°C. A helium pycnometer (Quantachrome-UltraFoam 1200e) was used to determine the true density of the samples and a particle size analyzer (Malvern Mastersizer) was used to monitor particle size distribution after suspending them in ethanol to deagglomerate the particles. The X-ray diffractogram (XRD) of the samples was recorded using an X-ray diffractometer (XRD Rigaku Miniflex 600 Advance) with Cu Kα radiation (1.5436 Å, 40 kV, 15 mA). The diffraction patterns were monitored in the 2θ range of 10–80° with an increment of $2°{\cdot}min^{-1}$. The bulk compositions of the samples were measured by XRF (Rigaku ZSX Primus) analysis while functional groups existing over the samples were detected via Fourier Transform Infrared Spectroscopy (Perkin Elmer, Spectrum 100) in the wavenumber range of 4000–400 cm^{-1}.

Alkali modification of FA

The modified materials used in this research were prepared in two steps which include microwave (MW) treatment and hydrothermal treatment in an alkaline medium at low temperature. The pulverized FA was soaked in an alkali solution in a flask and mixed for 1 h. For this purpose, 1 M NaOH solution was equally mixed with FA in a magnetic stirrer. The mixture was reacted under MW irradiation in an MW oven by setting the power at 800 W for 5 min of reaction time. Then the slurry was diluted up to a weight percentage of 50% with water and put in a Teflon container inside a stainless-steel autoclave vessel. The hydrothermal treatment was performed under autogenous pressure at 160°C for 12 h. Finally, the obtained mixture was filtered, washed with hot deionized water, and dried at 110°C.

Batch adsorption experiments

All chemicals used in batch adsorption studies were of analytical reagent grade and did not require further pre-treatment of purification stage. Metal solutions were made by dissolving the required amount of $Cu(NO_3)_2.3\,H_2O$ and $Cd(NO_3)_2.4\,H_2O$ in double deionized water to prepare 1000 mg/L Cu(II) and Cd(II) stock solutions, respectively. Stock solutions were prepared in standard concentrations of 1000 mg/L, which were diluted to desired concentration prior to adsorption experiments. For the batch adsorption experiments, the pH effect was not in the scope of the study and hence, the pH of the as-received solution was kept constant. All heavy metal adsorption experiments were performed in batch mode using a shaker at 200 rpm and the temperature was adjusted. When the residence time was over, the solution was filtered, and residual adsorbates concentrations were measured by an atomic absorption spectrometer (Perkin Elmer, Analyst 800). Experiments were performed to investigate the effects of adsorbent dose (1–6 g/L), initial metal ion concentration (200–600 mg/L), contact time (up to 600 min) and temperature (25–45°C). The uptake amount or quantity of metal adsorbed at a specific time (q_t) and equilibrium (q_e) were determined by using the equations listed below.

$$q_t = \frac{(C_i - C_t)}{w} xV \tag{1}$$

$$q_e = \frac{(C_i - C_e)}{w} xV \tag{2}$$

In the meanwhile, the adsorption percentage was obtained as follows:

$$Adsorption(\%) = \frac{(C_i - C_e)}{C_i} x100 \tag{3}$$

where C_i is the initial metal concentration (mg/L), C_e is the equilibrium metal concentration, (mg/L), C_t is the metal concentration at time t (mg/L), V is the volume of solution (L), and w is the mass of the sorbent (g).

Isotherm, kinetic, and thermodynamic analysis of adsorption data

Equilibrium modelling

Adsorption isotherms offer qualitative details about the interaction between the solute and the surface, including the correlation between the concentration of adsorbate and its degree of accumulation on the surface at a particular temperature. Achieving an optimal correlation for the equilibrium curves is necessary to design an effective sorption system. To model heavy metal adsorption, Langmuir, Freundlich, Dubinin–Radushkevich (D-R), and Temkin isotherm models were used in this study.

The Langmuir isotherm is based on physical and/or chemical interactions between the solute and accessible sites on the adsorbent's surface. The Langmuir equation is expressed in a linear form as follows:

$$\frac{C_e}{q_e} = \frac{1}{q_m K_L} + \frac{C_e}{q_m} \tag{4}$$

where q_m is the monolayer adsorption capacity (mg/g), and K_L is the Langmuir adsorption constant (L/mg).-[37,38] The affinity between adsorbate and adsorbent can be predicted using dimensionless separation factor (R_L). R_L is calculated as follows:

$$R_L = \frac{1}{1 + K_L C_o} \tag{5}$$

where C_o is the highest initial adsorbate concentration in the solution (mg/L). The R_L indicates whether the isotherm shape is unfavorable ($R_L > 1$), linear ($R_L = 1$), favorable ($0 < R_L < 1$) or irreversible ($R_L = 0$).[39]

Freundlich, in contrast to the Langmuir model, implies multilayer adsorbate absorption on the adsorbent surface (Freundlich, 1907). The following equation represents the linearized Freundlich isotherm:

$$\ln qe = \ln K_F + \frac{1}{n} \ln C_e \tag{6}$$

where K_F ($(mg/g)(L/mg)^{1/n}$) is a constant associated with the adsorption capacity and n is an empirical parameter.

The D-R isotherm is another empirical isotherm model that was first proposed for the sorption of subcritical vapors onto microporous sorbents using the pore filling [40] It implies that the adsorption potential varies across a heterogeneous surface.[41] The D-R isotherm equation has the following linear form:

$$\ln q_e = \ln q_m - \beta\varepsilon^2 \tag{7}$$

where β is a constant related to the adsorption energy (mol[2]/kJ,[2] q_m is the theoretical saturation capacity, and ε is the Polanyi potential. The Polanyi potential term can be calculated as given below:

$$\varepsilon = RT\left[1 + \frac{1}{C_e}\right] \tag{8}$$

where R is the gas constant (J/mol K) and T is the absolute temperature (K). And β constant of D-R equation gives the mean free energy E (kJ/mol) = $1/\sqrt{2\beta}$of adsorption per molecule of the adsorbate when it is transferred to the surface of the solid from infinity in the solution and can be calculated by the following equation:

$$E = \frac{1}{\sqrt{2\beta}} \tag{9}$$

The final isotherm model used in the study, Temkin[42,43] considers the effects of indirect adsorbent/adsorbate interactions and considers non-uniformly distributed sorbate-binding energies. The linear form of the Temkin isotherm equation is as follows:

$$q_e = B\ln K_T + B\ln C_e \tag{10}$$

To explore the adsorption isotherms, the same mass FA and N-FA were placed in different conical flasks containing 20 mL of heavy metal ions solution at concentrations of 200, 400, and 600 mg/L, respectively. The adsorption studies were carried out for 10 hours at 25°C.

Kinetic modelling

Batch adsorption data were also examined by pseudo-first order pseudo-second order and intraparticle diffusion and Elovich models to study adsorption mechanisms and derive kinetic parameters. Adsorption based on solid sorption capacity is primarily stated by a pseudo-first-order kinetic model [44] which considers that one metal ion is sorbed onto only a single sorption site. Lagergren's linearized pseudo-first-order rate equation is given as follows:

$$\log(q_e - q_t) = loq(q_e) - \frac{k_1 t}{2.303} \tag{11}$$

where k_1 is the pseudo-first order rate constant (1/min).

A pseudo-second-order equation[45] for expressing kinetics based on adsorption capacity is as follows:

$$\frac{t}{q_t} = \frac{1}{k_2 {q_e}^2} + \frac{1}{q_e}t \tag{12}$$

where k_2 is the pseudo-second order rate constant (g/mg.min).

It is well known that pseudo-first and pseudo-second order models cannot account for diffusion and rate limiting processes in the transport of sorbate molecules, the intraparticle diffusion model[46] is commonly used to satisfy this need. The intraparticle diffusion equation can be expressed as follows:

$$q_t = k_p t^{1/2} + C \tag{13}$$

where k_p is the intraparticle diffusion rate constant (mg/g $min^{1/2}$) and C is the intercept of model plot. If intraparticle diffusion is involved in the adsorption process, the plot should be straight, and if these lines pass through the origin, intraparticle diffusion is the rate-controlling step. Some degree of boundary layer control is assumed to exist when the plot does not pass through the origin. This suggests that intraparticle diffusion is not the only rate-limiting process, but that other kinetic models, due to their contribution to the overall transport of sorbate molecules, may also restrict the rate.[47]

Elovich kinetic model [48] may be suitable when the adsorbate ions and the surface sites interact chemically through a second-order mechanism. The linear form of Elovich equation can be represented by:

$$q_t = \frac{1}{\beta}\ln(\alpha\beta) + \frac{1}{\beta}\ln t \tag{14}$$

The adsorption kinetics were determined by immersing FA and N-FA of the same mass in different conical flasks holding 20 mL of 600 mg/L heavy metal ions solution at 25°C. The batch adsorption operation at duty was to determine the adsorption capacity of heavy metal ions absorbed at different contact times until equilibrium had been established.

Thermodynamic modelling

Thermodynamic parameters including Gibbs free energy change (ΔG°), enthalpy change (ΔH°), and entropy change (ΔS°) were frequently applied to analyze the effect of temperature and determine whether the adsorption process is spontaneous or not.

The Gibbs free energy change of the adsorption can be determined from the given equation:

$$\Delta G^o = -RT\ln K_L \tag{15}$$

where K_L is equilibrium constant which can be calculated using the following equation:

$$K_L = \frac{q_e}{C_e} \tag{16}$$

Relationship between ΔG°, ΔH° and ΔS° can be given by the following equation:

$$\Delta G^o = \Delta H^o - T\Delta S^o \tag{17}$$

Manipulation of Eq.15 provides the following linear equation for calculating thermodynamic parameters:

$$\ln K_L = -\frac{\Delta G^o}{RT} = -\frac{\Delta H^o}{RT} + \frac{\Delta S^o}{R} \tag{18}$$

Results and discussion

Effect of modification on the characteristics of fly ash

Textural characteristics

The success of adsorption process relies on an adsorbent with considerable surface area, pore volume, and appropriate functionalities.[49,50] Therefore, the relationships between their physical characteristics and surface chemistry of adsorbents must be critically assessed to maximize the economic and environmental benefits. A first analysis of the characteristics of the as-received and modified samples using the SEM technique revealed that morphology differed considerably due to the microwave-assisted hydrothermal treatment. As it is shown in Fig. 1, FA particles exhibited approximately spherical shapes and the sizes of the spherical particles ranged from less than 20 µm. Previous studies also showed that a typical FA that may be obtained combustion of coal includes microscopic spheres.[51] Apart from the untreated FA sample, the irregular particles of N-FA were non-spherical in shape. The applied modification procedure resulted in agglomerations of irregular shapes accompanied by a cracking of the sphericity of the FA which might introduce a few intrinsic pore formations.

According to the nitrogen adsorption-desorption isotherms, it was found that the surface area of the FA-N is greater than that of FA. Therefore, it can be concluded that the surface area of fly ash was increased by the modification possibly due to the cracking of the spherical structure and the formation of irregular cavities and unsmooth surfaces. The specific surface area of FA was found to be equal to 66.9 m^2/g while N-FA had a surface area of 123.4 m^2/g. The overall shape of the isotherms indicated hysteresis (Fig. 2). It is well known that the capillary condensation in mesopores is demonstrated by the development of hysteresis loops because of nitrogen adsorption and desorption.[52] After modification, the N-FA sample showed an H3 type of hysteresis formation which is characteristic of slit-shaped pores and is observed with non-rigid aggregates of plate-like particles[53]

In addition to nitrogen adsorption and desorption, Fig. 2 also represents the particle size distributions of the samples in ethanol dispersions that was monitored by a laser diffraction particle size analyzer. The bimodal curve of size dispersion shifted to the lower values after the modification. This corresponded to the particle size reduction due to the applied treatment process. According to the He pycnometer results of modified and unmodified fly ash, the real density was reduced due to the microwave-assisted hydrothermal treatment. The average values for FA and N-FA were 2.45 and 1.99 g/cm,[3] respectively. The introduction of new pores or enlargement of the existing pores in the FA may cause more void spaces within the material during modification and this may lead to a decrease in real density. The introduction of additional porosity through microwave-assisted alkali modification may slightly trade-off with the density of the fly ash. As more void spaces are created during the cracking of the spherical particles, the solid material occupies a smaller proportion of the total volume, resulting in a lower real density. Consequently, the modification method used in this study resulted in considerable changes in the textural characteristics of the material by altering particle shape, size, porosity, and density. This meant that the treatment method of modification generated a porous, less compact material than the starting fly ash material.

Compositional characteristics

The chemical composition and surface functional groups observed in the samples were thoroughly examined using comparative X-ray techniques together with FT-IR spectroscopy. The bulk compositions of the FA and N-FA were analyzed by XRF and the results are given in Table 1. The FA was consisted of mainly silicon dioxide (SiO_2), alumina (Al_2O_3), calcium oxide (CaO), and iron oxide (Fe_2O_3) phases, and the greatest portion in fly ash was determined to be SiO_2 accounting for 61.09 wt. % of the total. It was found that the amount decreased to 44.20 wt.%, while the amount of Al_2O_3 did not show so considerable change in weight percentage as SiO_2 did during modification. Based on this finding, the modification process altered the chemical composition of fly ash by promoting the alkali activation, dissolution, and leaching of SiO_2 due to the washout effect. It was also determined that the SiO_2/Al_2O_3 ratio decreased from 3.036 to 2.086 with the modification. There was also a significant decrease in the SiO_2/Na_2O ratio.

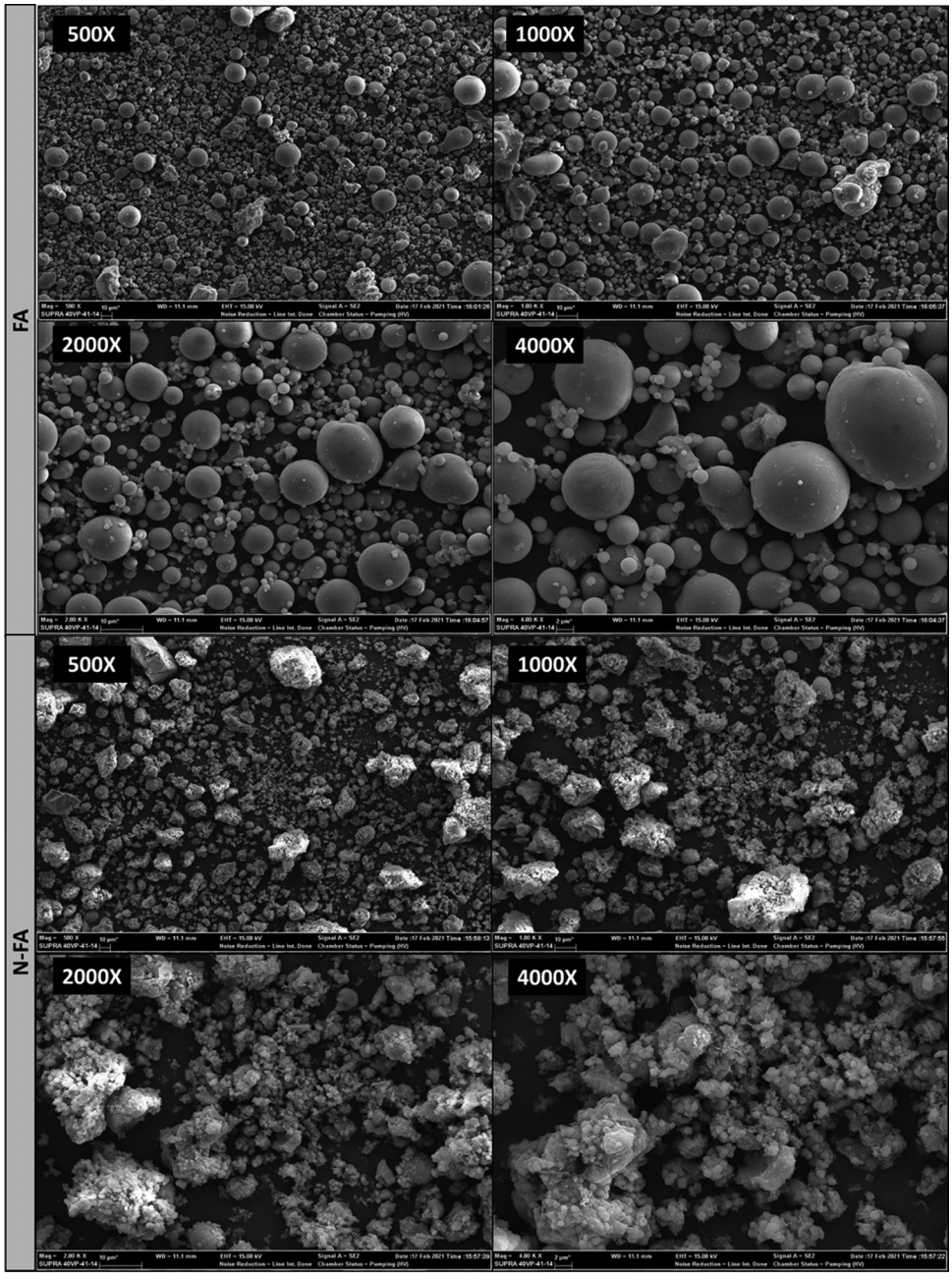

Figure 1. SEM micrographs of fly ash before (FA) and after (N-FA) treatment.

Figure 3 shows the X-ray powder diffraction patterns for FA and N-FA, where both materials contained a series of crystalline phases. After the modification of FA, the diffraction pattern varied noticeably as can be seen from the pattern of N-FA. The number of peaks detected by the integrator, and the structural constituents were identified by the search-match program. The figure shows the major contributor to the diffraction pattern was SiO_2, as it was also confirmed by XRF analysis. After microwave-assisted alkali hydrothermal treatment, the average crystallite size increased from 36.5 to 41.3 nm, which was calculated by Scherrer's equation. This may be explained by the dissolution of the amorphous components due to increased temperature in autogenous pressure during microwave-assisted alkali treatment. As a result, an increase in the average crystallite size was observed due to the rearrangement of the atoms in the crystalline lattice as they solidify, resulting in larger crystal structures.

FT-IR spectra of the samples were also analyzed to determine the effect of the microwave-assisted alkali modification process on the functional groups in the structure of the fly ash and were given in Fig. 4. It is well known that the existence of different functional groups

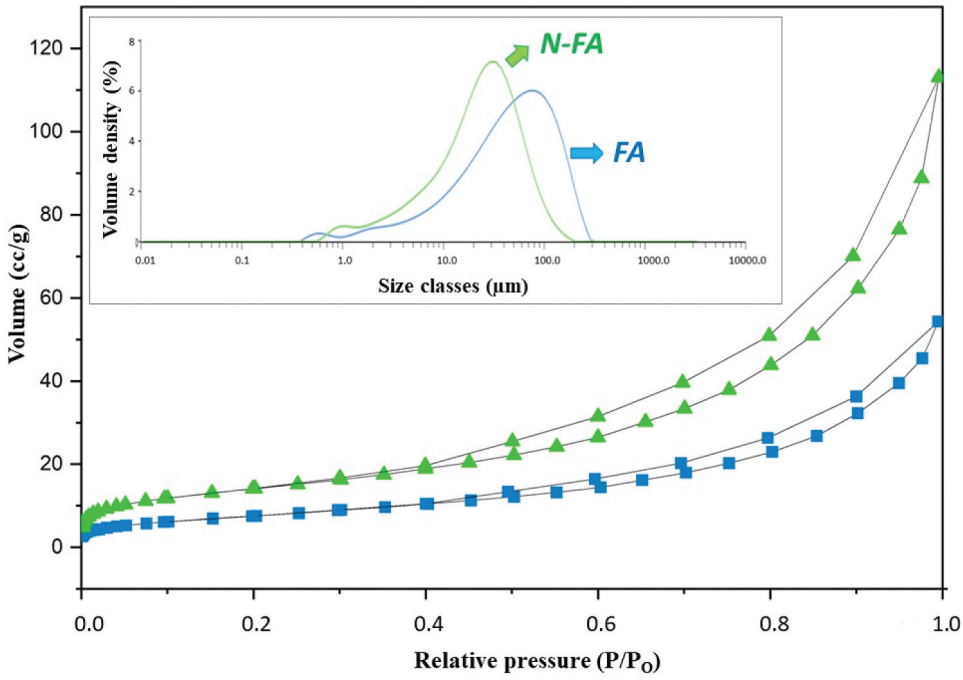

Figure 2. N_2 adsorption/desorption isotherms and particle size distributions of the adsorbents.

Table 1. Composition (wt.%) of the fly ash (FA) and alkali-modified fly ash (N-FA).

wt. %	FA	N-FA
SiO_2	61.09	44.20
Al_2O_3	20.12	21.18
CaO	4.90	5.44
Fe_2O_3	4.48	4.76
CO_2	2.63	11.92
K_2O	2.15	1.13
MgO	1.56	1.92
Na_2O	1.52	8.25
TiO_2	0.88	0.98
SO_3	0.46	0.04
BaO	0.21	0.18
SiO_2/Al_2O_3	***3.04***	***2.09***
SiO_2/Na_2O	***40.19***	***5.36***

on the surface of adsorbents creates some metal-binding regions.[54] For the FA, asymmetric stretching vibrations of Al-O and Si-O were observed around 1070 cm^{-1}. Furthermore, the band observed around 460 cm^{-1} corresponds to Al-O and Si-O internal deformation vibrations. The Si-O-Si and Al-O-Si symmetrical stretching vibrations are also known to be in the range of 778–750 cm^{-1}. With the modification, the intensities of asymmetric stretching vibrations of Al-O and Si-O and in-plane bending vibrations of Al-O and Si-O were decreased. Moreover, the – OH functional group observed around 3500 cm^{-1} and 1600 $cm^{-1}$was added to the structure after the treatment. The peaks observed between 1570 and 1350 cm^{-1} indicated the carbonation occurrence. These peaks appear in duplet form indicated that the carbonates were formed in different kinds of structures. To put it in other words, reactions involving the coupling of atmospheric carbon dioxide to hydroxides and hydrated aluminosilicates occurred during the treatment.

Heavy metal adsorption

The effect of several influential factors such as adsorbent dose, concentration, temperature, and contact time was initially investigated for batch adsorption of Cu(II) and Cd(VI) ions. Following that, systematic data analysis for equilibrium, kinetic, and thermodynamic modeling was performed.

Effect of adsorbent dose

Figure 5 depicts the heavy metal removal percent and adsorption capacity as a function of adsorbent dosage. In general, the removal rate of metal ions enhanced with increasing adsorption dosage, while adsorption capacity did not always increase. It is accepted that as the amount of adsorbent is increased, the adsorption sites of adsorbent remain unsaturated during the adsorption causing to decrease in adsorption capacity. But the aggregation/agglomeration of adsorbent particles at higher doses would not only cause a decrease in the available surface area but also prompt an increase in the diffusional path length.

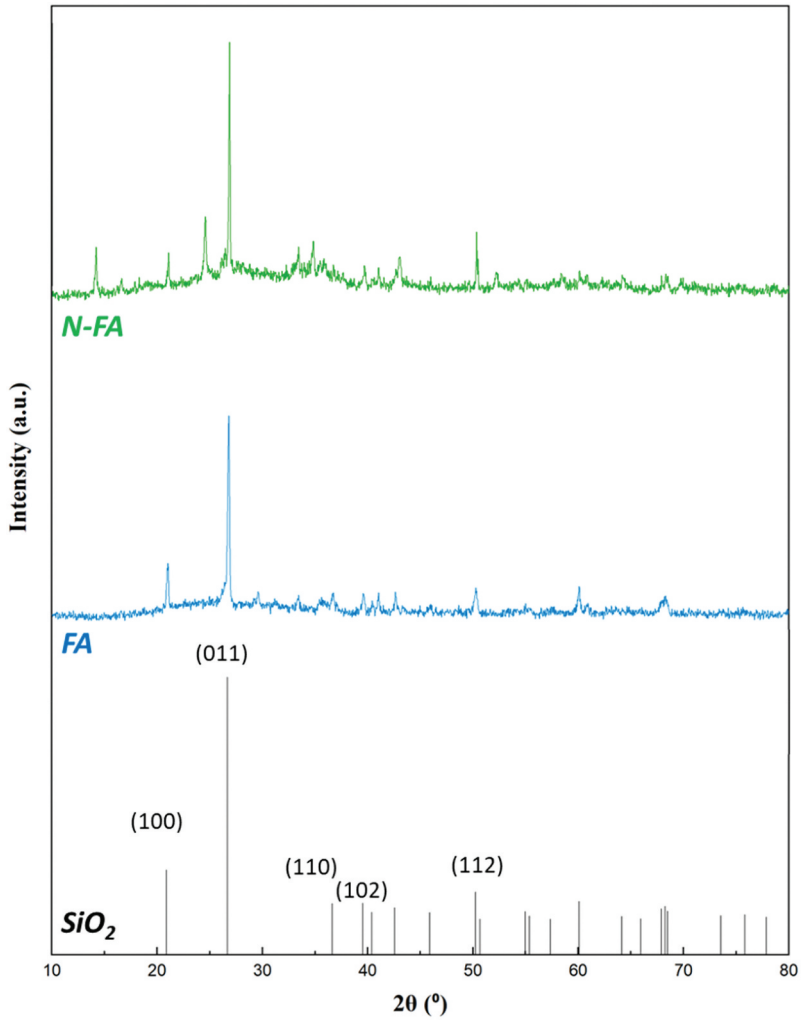

Figure 3. XRD patterns of the adsorbents.

Effect of initial heavy metal concentration, temperature, and contact time

Identifying the binding speed and determining the appropriate equilibrium time for the complete removal of heavy metal ions from the solution requires consideration of the important factor of contact time. It is accepted that the process efficiency decreases due to a saturation limit in the adsorption enhancement if the contact time of adsorption surpasses more than 4 hours.[55] As illustrated in Figure 6(a), each contact time versus q_t curve had a similar variation trend and the initial concentration of heavy metals in solution had a direct impact on adsorption capacity.[56] As shown in the figure, the adsorption capacity of FA and N-FA exhibited the same trend with the increase of adsorption time apart from the numerical values. In other words, up to a certain point, the Cd(II) and Cu(II) adsorption capacity increased with increasing initial heavy metal concentrations for both FA and N-FA sorbents. It is observed that at the initial stages of the process adsorption was fast as most of the surface of the sorbents was not saturated with metal ions. The effective adsorption sites on the adsorbent surface rapidly decreased as the Cd(II) and Cu(II) ions in the solution repelled those adsorbed on the adsorbent surface, and the adsorption rate declined in the later stages. As a result, the adsorption rate was initially rapid but eventually reduced due to saturation. Finally, an equilibrium between the adsorbate and the adsorbent surface was progressively achieved after 60 min for Cd(II) and Cu(II) ions. The adsorption equilibrium was reached a saturated adsorption of 99.7 and 109.4 mg/g, for FA and N-FA, respectively, at 600 mg/L initial Cd(II) concentration. The Cd(II) removal percentages at this equilibrium state were found to be 66.5% and 72.3%, for FA and N-FA, respectively. On the other hand, Cu(II) uptake was 52.9 and 80.2 mg/g for FA and N-FA, respectively, for an initial concentration of 600 mg/L at equilibrium. The percentages of Cu(II) removal at this equilibrium state were found to be 52.9% and 80.3% for

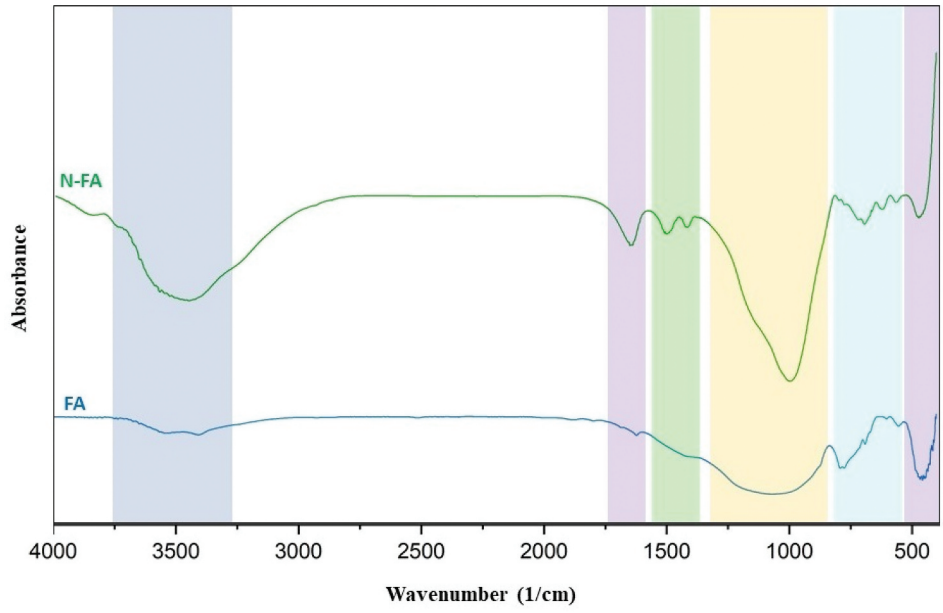

Figure 4. FT-IR spectra of the adsorbents.

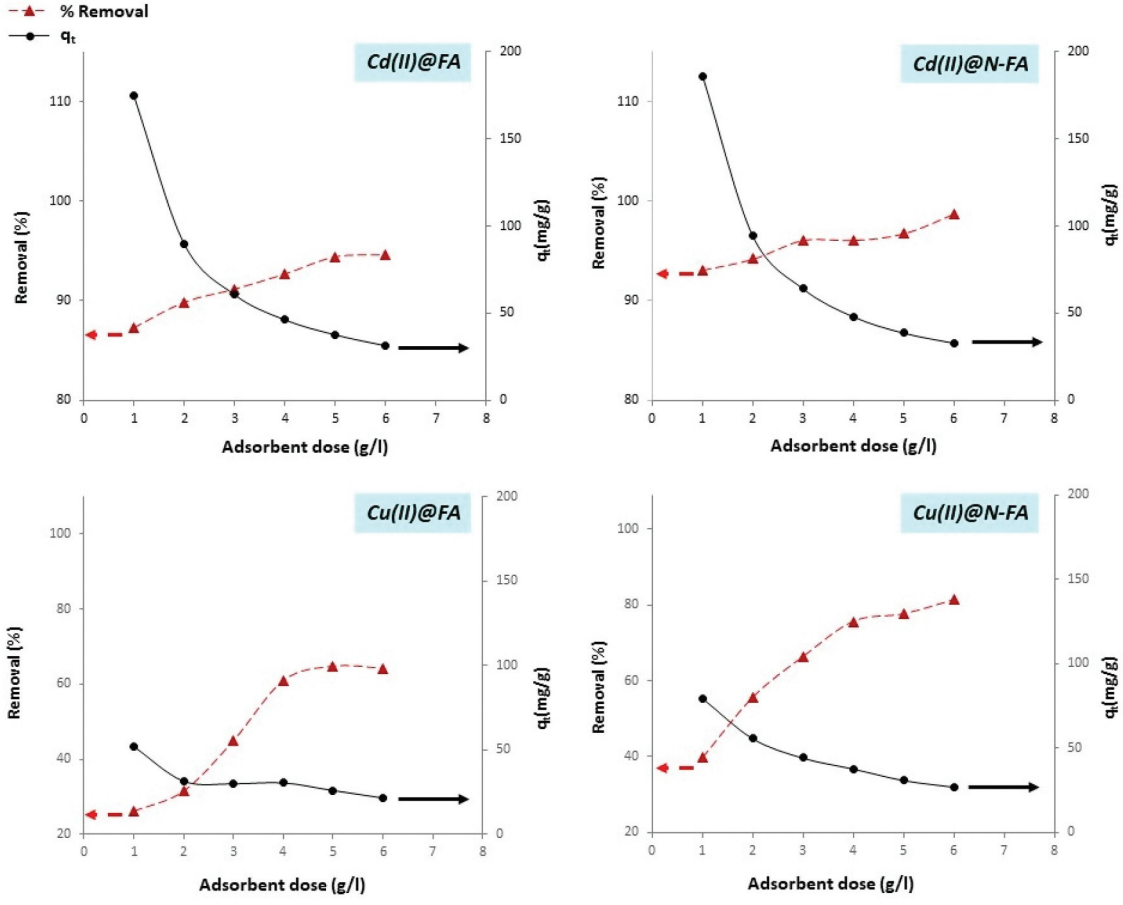

Figure 5. Effect of adsorbent dose for Cd(II) and Cu(II) adsorption. (Initial heavy metal concentration: 200 mg/L; contact time: 120 min; temperature: 25°C)

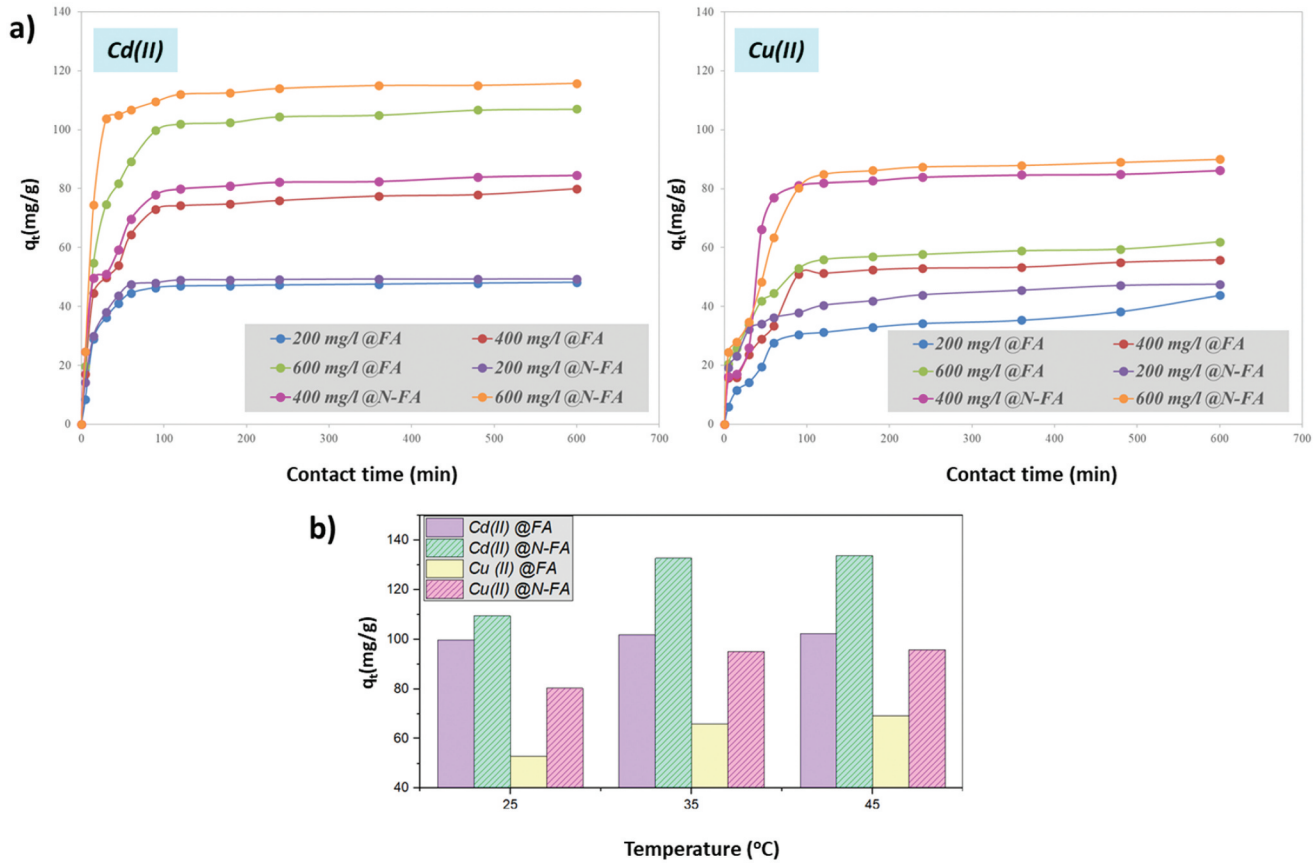

Figure 6. Effect of heavy metal concentration and contact *time (temperature:25°C; adsorbent dose: 4 g/L)* (a) and temperature *(initial heavy metal concentration: 600 mg/L; adsorbent dose: 4 g/L; contact time:90 mins)* (b).

FA and N-FA, respectively. When the adsorption capacity did not increase, the adsorption remained in a state of dynamic equilibrium. There was no considerable change after this equilibrium state for all initial concentrations of both ions (which are changing from 200 to 600 mg/L), because adsorption sites were mostly occupied. When the effect of initial heavy metal concentration was critically analyzed, it was seen that metal uptake was enhanced by increasing initial concentrations for all cases. A possible explanation may be that increasing the concentration of metal ions in solution induces an increase in mass transfer because the driving force for transporting ions from solution to sorbent increases. The initial high concentration boosts the mass transfer of sorbate metal ions onto the adsorbent's surfaces, since the surfaces are saturated with enough heavy metal, the interactions of those free heavy metals with adsorbents would be hindered[55]

Another significant factor that may influence the adsorption of heavy metals is temperature, which may do so by influencing solubility and molecular interactions with solid particles. The adsorption was also studied at different temperatures, and it is found that the adsorption capacity of ions increased at higher temperatures Figure 6(b). These may be attributed to the endothermicity of Cu(II) and Cd(II) adsorption as will be further supported by thermodynamic analysis. At the conditions employed, maximum adsorption capacities were obtained at 45°C. The highest sorption capacities were obtained in the case of using a modified form of fly ash (N-FA) at the highest temperature. This could be attributed to the development of increased sorption sites on fly ash or an increase in heavy metal diffusion into adsorbent pores at high temperatures. Consequently, after 90 minutes, for Cd(II) and Cu(II), the adsorption capacity progressively increased. Moreover, the adsorption capacity of sorbents was found different for Cd(II) and Cu(II) ions, which means they are affected by the accessibility of binding sites and ionic charge repulsion. The highest adsorption of N-FA was achieved as 133.8 and 95.7 mg/g for Cd(II) and Cu(II), respectively, at 600 mg/L initial heavy metal concentration, 600 min contact time, and 45°C. These values were 102.2 and 69.1 for the unmodified fly ash at 600 mg/L initial heavy metal concentration, 600 min contact time, and 45°C.

Adsorption isotherms

Based on the data gained from batch adsorption experiments, a careful examination of isotherm modeling was performed to comprehend the mechanism and forecast the behavior of the system. To enable the precise fitting of the equilibrium data, several models were used including Langmuir, Freundlich, Dubinin–Radushkevich (D-R), and Temkin, and the results were summarized in Table 2. Regression coefficient values obtained by fitting the experimental results onto Freundlich model were obviously between 0.9805 and 0.9988, which was better than that of Langmuir, DR, and Temkin models. The values of the regression coefficient are a criterion of fitting, demonstrating that the Freundlich model adequately describes the experimental data of Cd(II) and Cu(II). The heterogeneous adsorption process can be explained using the Freundlich adsorption isotherm model, which accounts for the multilayer adsorption of the adsorbate on surfaces that are heterogeneous and have varying energies.[57,58] This model considers the adsorption sites possess different binding energies, resulting in the non-uniformity of the adsorption process [59,60] K_F and *n* values listed in the isotherm table are the Freundlich model parameter and the intensity of adsorption linked to adsorption capacity, respectively. When the value of 1/n is less than unity, it represents a typical favorable adsorption process, and the adsorption energy declines as the surface concentration increases.[61] The numerical values of Freundlich parameters (K_F) indicate that the highest heavy metal removal efficiency is achieved when the modified fly ash was used in Cd(II) removal process from aqueous solutions. As a result, the Cd(II) and Cu(II) adsorption corresponded to the adsorption of active sites with varied energies based on multiple layers on heterogeneous surfaces of both unmodified and modified fly ash. Furthermore, the modification of FA changed the isotherm significantly as it is given in the table. According to the comparative evaluation, FA has good adsorption efficiency for the adsorption of Cd(II), and it may be increased further through microwave-assisted alkali hydrothermal modification process.

Adsorption kinetics

The process of adsorption requires a correct expression of the reaction rate and sorption mechanism to understand how quickly a solute is absorbed. This mechanism encompasses mass transfer, diffusion, and the reaction occurring on the surface of the adsorbent during the adsorption process.[62] Kinetics which occurs at constant concentration and can be linear or non-linear is used to determine the rate at which metal ions are released from the solution and diffuse in the pores of the solid interface [63] Using kinetic models and investigating the rate-controlling mechanisms, the process of removing Cd(II) and Cu(II) ions from an aqueous phase by FA and N-FA can be explained and the adsorption rate may be estimated to design and model the larger-scale adsorption operations. For the studied adsorbent-adsorbate systems, kinetic analysis was performed using four different models, and the obtained results are given in Table 3. The regression coefficient values of all cases for the pseudo-second-order model were higher than those calculated by the other three models. As a consequence, the analysis of different adsorption kinetic models revealed that the adsorption of Cd(II) and Cu(II) was primarily chemical, which was more compatible with the pseudo-second-order kinetic model. This behavior of heavy metal adsorption is due to a chemisorption-

Table 2. Isotherm constants for adsorption of Cd(II) and Cu(II) at 25°C.

	Cd(II)		*Cu(II)*	
Isotherm	FA	N-FA	FA	N-FA
Langmuir				
q_m (mg/g)	116.3	121.9	76.9	82.6
K_L (l/mg)	0.0229	0.0375	0.0104	0.0816
R^2	0.9622	0.9765	0.9965	0.9945
Freundlich				
K_F ((mg/g) (L/mg)$^{1/n}$)	16.7	24.5	6.7	35.9
n	3.0	3.2	2.6	3.1
R^2	0.9805	0.9886	0.9988	0.9948
Dubinin–Radushkevich				
q_m (mg/g)	86.7	94.2	58.1	74.5
β	$4.0x10^{-5}$	$1.0x10^{-5}$	$4.0x10^{-4}$	$5.0x10^{-6}$
E	$1.1x10^{[2]}$	$2.2x10^{[2]}$	3.5x10	$3.2x10^{[2]}$
R^2	0.8629	0.8793	0.9427	0.9198
Temkin				
B	22.6	22.2	16.9	29.8
K_T	0.3218	0.6493	0.1008	0.3274
R^2	0.9427	0.9629	0.9982	0.9724

Table 3. Kinetic parameters for adsorption of Cd(II) and Cu(II) (at 25°C and 600 mg/l initial heavy metal concentration).

	Cd(II)		*Cu(II)*	
Kinetic Model	FA	N-FA	FA	N-FA
Pseudo-first order				
k_1	0.0347	0.0616	0.0269	0.0221
q_e	81.5	87.9	39.4	72.7
R^2	0.9824	0.9014	0.9892	0.9939
Pseudo-second order				
k_2	0.0005	0.0004	0.0014	0.0003
q_e	117.6	135.1	53.8	91.7
R^2	0.9943	0.9793	0.9930	0.9964
Intraparticle diffusion				
k_p	11.8	13.1	5.1	8.6
C	2.9	12.4	6.4	5.3
R^2	0.9442	0.8506	0.9842	0.9930
Elovich				
α	13.1	19.3	9.2	6.8
β	0.0372	0.0311	0.0876	0.0521
R^2	0.9951	0.9471	0.9869	0.9890

dependent rate-determining step which involves valence forces through the sharing or exchange of electrons between the sorbent and sorbate, along with complexation, coordination, and/or chelation[64] This pseudo-second order model also indicates that as the initial concentration of metal ions and adsorbent doses increase, so does the adsorption capacity.[65] Moreover, the pseudo-second-order reaction implies that the rate of adsorption is related to the number of unoccupied sites on the surface.[66,67] The q_e values calculated using the pseudo-second-order models were 117.6 mg Cd(II)/g FA, 135.1 mg Cd(II)/g N-FA, and 53.8 mg Cu(II)/g FA and 91.7 mg Cu(II)/g N-FA which were in alignment with the values obtained from previous experiments.

Moreover, the lower value of the k_2 parameter calculated by pseudo-second-order model indicates adsorption affinity was increased for both Cd(II) and Cu(II) ions after modification. Therefore, it is convenient to say that the results of this kinetics modeling are exactly aligned with the Cd(II) and Cu(II) adsorption capability of both FA and N-FA.

Table 4. Thermodynamic parameters of Cd(II) and Cu(II) adsorption.

Adsorbent	Metal ion	T (°C)	ΔG° (kj/mol)	ΔH° (kj/mol)	ΔS° (j/mol K)	R^2
FA	Cu(II)	20	−16.1	34.1	167.9	0.9852
		30	−17.5			
		40	−19.4			
	Cd(II)	20	−19.5	18.4	126.8	0.9891
		30	−20.6			
		40	−22.0			
N-FA	Cu(II)	20	−21.2			
		30	−22.4	16.2	125.4	0.9993
		40	−23.6			
	Cd(II)	20	−20.6			
		30	−22.2	22.7	145.7	0.9917
		40	−23.6			

Adsorption thermodynamics

Thermodynamic parameters are the subject of scientific assessments which elucidate adsorption mechanisms, which can then be used to modify and optimize processes with enhanced efficiency. To find out the spontaneity, the parameters such as entropy (ΔS°), Gibbs free energy (ΔG°), and enthalpy (ΔH°) can be determined. Sorption increases in endothermic systems and decreases in exothermic systems, depending on the thermodynamics of the adsorption. According to the results given in Table 4, ΔH ° values of each investigated adsorbent-adsorbate system were found to be positive, indicating endothermicity of the adsorption processes.[68] The ΔS° values for all metal ions demonstrate the affinity of adsorbents toward heavy metal ions which may be due to increasing randomness at the solid/solution interface throughout the heavy metal removal process.[69,70] The negative ΔG° values suggested that both Cd(II) and Cu(II) adsorption onto FA and N-FA was thermodynamically feasible and spontaneous. The decline in ΔG° values with increasing temperature implied favored adsorption feasibility at higher temperatures for both ions. Moreover, the microwave-assisted hydrothermal treatment decreased the ΔG° values for both adsorption of Cd(II) and Cu(II) ions at each temperature due to the increased availability of adsorption sites.

Table 5. Comparison of the performance of sorbents for Cu(II) and Cd(II) adsorption.

Adsorbent	Heavy metal	Adsorption capacity (mg/g)	Isotherm fitting	Kinetic model	Temperature dependency	Reference
Mecanically activated fly ash	Cu(II)	98.7	Langmuir	Pseudo-2nd order	Endothermic	[71]
Alkali activated fly ash	Cu(II)	152.2	Langmuir	Pseudo-2nd order	Endothermic	[72]
Metal Oxide-Modified Fly Ash	Cd(II)	~160	Langmuir	N/A	N/A	[73]
Coal fly ash	Cu(II)	20.9	Langmuir	Pseudo-2nd order	N/A	[74]
	Cd(II)	18.8				
Chitosan coated fly ash	Cu(II)	28.5	Freundlich	Pseudo-2nd order	Endothermic	[75]
Acid activated kaolinite and montmorillonite	Cu(II)	21.9	Langmuir	Pseudo-2nd order	Endothermic	[76]
Barley straw ash	Cu(II)	~10.0	Combined Langmuir& Freundlich	Pseudo-2nd order	Endothermic	[77]
	Cd(II)	~5.5				
PV glass-fly ash composite	Cu(II)	60.1	Langmuir	Pseudo-2nd order	N/A	[78]
	Cd(II)	55.5				
Alkali treated coal fly ash	Cd(II)	79.8	Langmuir	Pseudo-2nd order	N/A	[79]
Hydrothermally modified fly ash	Cu(II)	56.4	Langmuir	Pseudo-2nd order	N/A	[33]
	Cd(II)	87.7				
FA	Cu(II)	69.1	Freundlich	Pseudo-2nd order	Endothermic	This study
	Cd(II)	102.2				
N-FA	Cu(II)	95.7				
	Cd(II)	133.8				

*N/A: not available.

Table 5 shows that Cu(II) and Cd(II) ions could be adsorbed by various ash and fly-ash-based sorbents and a comparison of the current study has been made with the literature findings. It can be concluded that, both the characteristics of the ashes and the conditions of the adsorption process have a marked effect on capacity, equilibrium, kinetics, and thermodynamics. According to the table, among the sorbents identified in the literature, N-FA is believed to be appealing for the removal of heavy metal ions with reasonable adsorptive capacities toward Cu(II) and Cd(II) ions.

Conclusions

In this work, the effect of microwave-assisted hydrothermal treatment in the alkaline medium on the characteristics of fly ash was investigated and the batch adsorption of Cd(II) and Cu(II) was further studied using both modified and unmodified samples. The MW treatment affected the particle size and surface properties of FA by reducing the particle size and deforming the surface to increase porosity and surface area by approximately two folds. The batch adsorption study was performed to explore the effect of adsorbent dose, contact time, initial metal ion concentration, and temperature on adsorption behavior. The adsorption capacity for Cd(II) was higher than Cu(II) for modified and unmodified samples, which indicated that adsorbent–adsorbate interaction plays a major role in the removal mechanism of heavy metals. Comparing the regression coefficients reveals that the sorption of Cd(II) and Cu(II) onto the FA, and N-FA can be successfully described by the Freundlich isotherm model, while the kinetic behavior of the adsorbent-adsorbate systems can be explained by pseudo-second-order kinetics. Our findings corroborate by stating that modified fly ash, when utilized as a low-cost adsorbent, could be promising for wastewater remediation processes since we envisage that our findings are also applicable to other heavy metal adsorption processes.

Acknowledgments

We thank Dinçer Cement Ind. for supplying fly ash sample, Dr. Murat Kılıç for helping the particle size analysis, and Abdullah Düzgün for helping atomic absorption spectroscopy analyses.

Disclosure statement

No potential conflict of interest was reported by the author(s).

References

[1] Chugh, M.; Kumar, L.; Shah, M. P.; Bharadvaja, N. Algal Bioremediation of Heavy Metals: An Insight into Removal Mechanisms, Recovery of By-Products, Challenges, and Future Opportunities. *Energy Nexus*. 2022, *7*, 100129. DOI: 10.1016/j.nexus.2022.100129.

[2] Hong, H. J.; Ryu, J. Synthesis of Copper Nanoparticles from Cu2±spiked Wastewater via Adsorptive Separation and Subsequent Chemical Reduction. *Nanomaterials*. 2021, *11*(8), 2051. DOI: 10.3390/nano11082051.

[3] Wang, F.; Wang, F.; Yang, H.; Yu, J.; Ni, R. Ecological Risk Assessment Based on Soil Adsorption Capacity for Heavy Metals in Taihu Basin, China. *Environ. Pollut*. 2023, *316*, 120608. DOI: 10.1016/j.envpol.2022.120608.

[4] Chakraborty, R.; Asthana, A.; Singh, A. K.; Jain, B.; Susan, A. B. H. Adsorption of Heavy Metal Ions by Various Low-Cost Adsorbents: A Review. *Int. J. Environ. Anal. Chem*. 2022, *102*(2), 342–379. DOI: 10.1080/03067319.2020.1722811.

[5] Arief, V. O.; Trilestari, K.; Sunarso, J.; Indraswati, N.; Ismadji, S. Recent Progress on Biosorption of Heavy Metals from Liquids Using Low Cost Biosorbents: Characterization, Biosorption Parameters and Mechanism Studies. *Clean (Weinh)*. 2008, *36*(12), 937–962. DOI: 10.1002/clen.200800167.

[6] Ryu, J.; Kim, S.; Hong, H. J.; Hong, J.; Kim, M.; Ryu, T.; Park, I.-S.; Chung, K.-S.; Jang, J. S.; Kim, B.-G., et al. Strontium Ion (Sr2+) Separation from Seawater by Hydrothermally Structured Titanate Nanotubes: Removal Vs. Recovery. *Chem. Eng. J*. 2016, *304*, 503–510. DOI: 10.1016/j.cej.2016.06.131.

[7] Hu, J.; Zhang, L.; Yu, Y.; Liang, C.; Sang, Y. Selective Extraction of Heavy Metals from Sewage Sludge via Combined Process of Acid Leaching and Ion Exchange Resins Adsorption: Optimization and Performance Evaluation. *Sep. Sci. Technol*. 2023, *58*(10), 1773–1783. DOI: 10.1080/01496395.2023.2215400.

[8] Sultana, M.; Rownok, M. H.; Sabrin, M.; Rahaman, M. H.; Alam, S. M. N. A Review on Experimental Chemically Modified Activated Carbon to Enhance Dye and Heavy Metals Adsorption. *Clean Eng. Technol*. 2022, *6*, 100382. DOI: 10.1016/j.clet.2021.100382.

[9] Chirenje, T.; Ma, L. Q.; Lu, L. Retention of Cd, Cu, Pb and Zn by Wood Ash, Lime and Fume Dust. *Water Air Soil Pollut*. 2006, *171*(1–4), 301–314. DOI: 10.1007/s11270-005-9051-4.

[10] Li, S.; Yang, L.; Wu, J.; Yao, L.; Han, D.; Liang, Y.; Yin, Y.; Hu, L.; Shi, J.; Jiang, G., et al. Efficient and Selective Removal of Hg(ii) from Water Using Recyclable Hierarchical MoS2/Fe3O4 Nanocomposites. *Water Res*. 2023, *235*, 119896. DOI: 10.1016/j.watres.2023.119896.

[11] Li, W.; Sun, Y.; Sun, H.; Zhang, S.; Wang, F. A Novel Clay/sludge-Based Magnetic Ceramsite: Preparation and Adsorption Removal for Aqueous Cu(ii). *Sep. Sci. Technol*. 2023, *58*(9), 1565–1582. DOI: 10.1080/01496395.2023.2203326.

[12] Morosanu, I.; Paduraru, C.; Bucatariu, F.; Fighir, D.; Mihai, M.; Teodosiu, C. Shaping Polyelectrolyte Composites for Heavy Metals Adsorption from Wastewater: Experimental Assessment and Equilibrium Studies. *J. Environ. Manage*. 2022, *321*, 115999. DOI: 10.1016/j.jenvman.2022.115999.

[13] Tang, W. W.; Zeng, G. M.; Gong, J. L.; Liang, J.; Xu, P.; Zhang, C.; Huang, B.-B. Impact of Humic/Fulvic Acid on the Removal of Heavy Metals from Aqueous Solutions Using Nanomaterials: A Review. *Sci. Total Environ*. 2014, *468-469*, 1014–1027. DOI: 10.1016/j.scitotenv.2013.09.044.

[14] Manyangadze, M.; Chikuruwo, N. H. M.; Narsaiah, T. B.; Chakra, C. S.; Radhakumari, M.; Danha, G. Enhancing Adsorption Capacity of Nano-Adsorbents via Surface Modification: A Review. *S. Afr. J. Chem. Eng*. 2020, *31*, 25–32. DOI: 10.1016/j.sajce.2019.11.003.

[15] He, X.; Deng, F.; Shen, T.; Yang, L.; Chen, D.; Luo, J. Exceptional Adsorption of Arsenic by Zirconium Metal-Organic Frameworks: Engineering Exploration and Mechanism Insight. *J. Colloid. Interface. Sci*. 2019, *539*, 223–234. DOI: 10.1016/j.jcis.2018.12.065.

[16] Wang, M.; Zeng, M.; Wang, P.; Liu, Y. Comparative Investigation on Ni(ii) Removal from Electroplating Wastewater by Mineral Adsorbent (CSAM) and Ion-Exchange Resins. *Sep. Sci. Technol*. 2023, *58*(11), 1959–1971. DOI: 10.1080/01496395.2023.2223754.

[17] Liu, D.; Ding, C.; Chi, F.; Pan, N.; Wen, J.; Xiong, J.; Hu, S. Polymer Brushes on Graphene Oxide for Efficient Adsorption of Heavy Metal Ions from Water. *J. Appl. Polym. Sci*. 2019, *136*(43), 48156. DOI: 10.1002/app.48156.

[18] Putra, E. K.; Pranowo, R.; Sunarso, J.; Indraswati, N.; Ismadji, S. Performance of Activated Carbon and Bentonite for Adsorption of Amoxicillin from Wastewater: Mechanisms, Isotherms and Kinetics. *Water Res*. 2009, *43*(9), 2419–2430. DOI: 10.1016/j.watres.2009.02.039.

[19] Mahdi, Z.; Yu, Q. J.; El Hanandeh, A. Competitive Adsorption of Heavy Metal Ions (Pb^{2+}, Cu^{2+}, and Ni^{2+}) Onto Date Seed Biochar: Batch and Fixed Bed Experiments. *Sep. Sci. Technol*. 2019, *54*(6), 888–901. DOI: 10.1080/01496395.2018.1523192.

[20] Sriram, G.; Kigga, M.; Uthappa, U. T.; Rego, R. M.; Thendral, V.; Kumeria, T.; Jung, H.-Y.; Kurkuri, M. D. Naturally Available Diatomite and Their Surface Modification for the Removal of Hazardous Dye and Metal Ions: A Review. *Adv. Colloid Interface Sci*. 2020, *282*, 102198. DOI: 10.1016/j.cis.2020.102198.

[21] Choi, H. D.; Jung, W. S.; Cho, J. M.; Ryu, B. G.; Yang, J. S.; Baek, K. Adsorption of Cr(vi) Onto Cationic Surfactant-Modified Activated Carbon. *J. Hazard. Mater*. 2009, *166*(2–3), 642–646. DOI: 10.1016/j.jhazmat.2008.11.076.

[22] Zhou, Y.; Zhang, R.; Gu, X.; Lu, J. Adsorption of Divalent Heavy Metal Ions from Aqueous Solution by Citric Acid Modified Pine Sawdust. *Sep. Sci. Technol*. 2015, *50*(2), 245–252. DOI: 10.1080/01496395.2014.956223.

[23] Hashem, M. A.; Mim, S.; Payel, S.; Shaikh Md, M. Z. R.; Nur-A-Tomal Md, S. Comparative Chromium Adsorption Studies on Thermally and Chemical-Thermally Modified Ficus Carica Adsorbents. *Int. J. Environ. Sci. Technol*. Published online February 13, 2023; *20* 11, 12363–12378. DOI:10.1007/s13762-023-04806-y.

[24] Shyam, R.; Puri, J. K.; Kaur, H.; Amutha, R.; Kapila, A. Single and Binary Adsorption of Heavy Metals on Fly Ash Samples from Aqueous Solution. *J. Mol. Liq*. 2013, *178*, 31–36. DOI: 10.1016/j.molliq.2012.10.031.

[25] Mishra, A.; Tripathi, B. D. Utilization of Fly Ash in Adsorption of Heavy Metals from Wastewater. *Toxicol. Environ. Chem*. 2008, *90*(6), 1091–1097. DOI: 10.1080/02772240801936786.

[26] Alinnor, I. J. Adsorption of Heavy Metal Ions from Aqueous Solution by Fly Ash. *Fuel*. 2007, *86*(5–6), 853–857. DOI: 10.1016/j.fuel.2006.08.019.

[27] Kumar, M.; Goswami, L.; Singh, A. K.; Sikandar, M. Valorization of Coal Fired-Fly Ash for Potential Heavy Metal Removal from the Single and Multi-Contaminated System. *Heliyon*. 2019, *5*(10), e02562. DOI: 10.1016/j.heliyon.2019.e02562.

[28] Onder, A.; Ilgin, P.; Ozay, H.; Ozay, O. Preparation of Composite Hydrogels Containing Fly Ash as Low-Cost Adsorbent Material and Its Use in Dye Adsorption. *Int. J. Environ. Sci. Technol*. 2022, *19*(8), 7031–7048. DOI: 10.1007/s13762-021-03622-6.

[29] Aigbe, U. O.; Ukhurebor, K. E.; Onyancha, R. B.; Osibote, O. A.; Darmokoesoemo, H.; Kusuma, H. S. Fly Ash-Based Adsorbent for Adsorption of Heavy Metals and Dyes from Aqueous Solution: A Review. *J. Mater. Res. Technol*. 2021, *14*, 2751–2774. DOI: 10.1016/j.jmrt.2021.07.140.

[30] Zhuang, X. Y.; Chen, L.; Komarneni, S.; Zhou, C. H.; Tong, D. S.; Yang, H. M.; Yu, W. H.; Wang, H. Fly Ash-Based Geopolymer: Clean Production, Properties and Applications. *J. Clean. Prod*. 2016, *125*, 253–267. DOI: 10.1016/j.jclepro.2016.03.019.

[31] Więckowski, M.; Dudzińska, A. Impact of Using Fly and Bottom Ash on Fire Risk Assessment in Hard Coal Mines. *Int. J. Environ. Sci. Technol*. 2023, *20*(1), 75–86. DOI: 10.1007/s13762-022-03991-6.

[32] Caetano, A. P. F.; Carvalheiras, J.; Senff, L.; Seabra, M. P.; Pullar, R. C.; Labrincha, J. A.; Novais, R. M. Unravelling the Affinity of Alkali-Activated Fly Ash Cubic Foams Towards Heavy Metals Sorption. *Materials*. 2022, *15*(4), 1453. DOI: 10.3390/ma15041453.

[33] Visa, M.; Chelaru, A. M. Hydrothermally Modified Fly Ash for Heavy Metals and Dyes Removal in Advanced Wastewater Treatment. *Appl. Surf. Sci*. 2014, *303*, 14–22. DOI: 10.1016/j.apsusc.2014.02.025.

[34] Nascimento, M.; Soares, P. S. M.; Souza, V. P. D. Adsorption of Heavy Metal Cations Using Coal Fly Ash Modified by Hydrothermal Method. *Fuel*. 2009, *88*(9), 1714–1719. DOI: 10.1016/j.fuel.2009.01.007.

[35] Zhou, Q.; Jiang, X.; Qiu, Q.; Zhao, Y.; Long, L. Synthesis of High-Quality Na P1 Zeolite from Municipal Solid Waste Incineration Fly Ash by Microwave-Assisted Hydrothermal Method and Its Adsorption Capacity.

Sci. Total Environ. 2023, *855*, 158741. DOI: 10.1016/j.scitotenv.2022.158741.

[36] Zhang, J.; Chen, T.; Li, H.; Tu, S.; Zhang, L.; Hao, T.; Yan, B. Mineral Phase Transition Characteristics and Its Effects on the Stabilization of Heavy Metals in Industrial Hazardous Wastes Incineration (IHWI) Fly Ash via Microwave-Assisted Hydrothermal Treatment. *Sci. Total Environ.* 2023, *877*, 162842. DOI: 10.1016/j.scitotenv.2023.162842.

[37] Langmuir, I. The Adsorption of Gases on Plane Surfaces of Glass, Mica and Platinum. *J. Am. Chem. Soc.* 1918, *40*(9), 1361–1403. DOI: 10.1021/ja02242a004.

[38] Langmuir, I. The constitution and fundamental properties of solids and liquids. II. Liquids. [1]. *J. Am. Chem. Soc.* 1917, *39*(9), 1848–1906. DOI: 10.1021/ja02254a006.

[39] Freundlich, H. Über die Adsorption in Lösungen. *Zeitschrift für Physikalische Chemie*. 1907, *57U*(1), 385–470. DOI: 10.1515/zpch-1907-5723.

[40] Tang, X. W.; Li, Z. Z.; Chen, Y. M.; Wang, Y. Removal of Cu(ii) from Aqueous Solution by Adsorption on Chinese Quaternary Loess: Kinetics and Equilibrium Studies. *J. Environ. Sci. Health A.* 2008, *43*(7), 779–791. DOI: 10.1080/10934520801960144.

[41] Dubinin, M. M. The Equation of the Characteristic Curve of Activated Charcoal. *Dokl. Akad. Nauk. SSSR.* 1947, *55*, 327–329.

[42] Temkin, M. I. Kinetics of Ammonia Synthesis on Promoted Iron Catalysts. *Acta physiochim URSS.* 1940, *12*, 327–356.

[43] Temkin, M. J.; Pyzhev, V. Recent Modifications to Langmuir Isotherms. Published online 1940.

[44] Lagergren, S. K. About the Theory of So-Called Adsorption of Soluble Substances. *Sven. Vetenskapsakad. Handingarl.* 1898, *24*, 1–39.

[45] Ho, Y. S.; McKay, G. Pseudo-Second Order Model for Sorption Processes. *Process Biochem.* 1999, *34*(5), 451–465. DOI: 10.1016/S0032-9592(98)00112-5.

[46] Weber, W. J., Jr; Morris, J. C. Kinetics of Adsorption on Carbon from Solution. *J. Sanitary Eng. Div.* 1963, *89*(2), 31–59. DOI: 10.1061/JSEDAI.0000430.

[47] Chen, J. P.; Wu, S.; Chong, K. H. Surface Modification of a Granular Activated Carbon by Citric Acid for Enhancement of Copper Adsorption. *Carbon.* 2003, *41* (10), 1979–1986. DOI: 10.1016/S0008-6223(03)00197-0.

[48] Elovich, S. Y.; Larionov, O. G. Theory of Adsorption from Nonelectrolyte Solutions on Solid Adsorbents. *Bull. Acad. Sci. USSR Div. Chem. Sci.* 1962, *11*(2), 198–203. DOI: 10.1007/BF00908017.

[49] Wang, S.; Sun, H.; Ang, H. M.; Tadé, M. O. Adsorptive Remediation of Environmental Pollutants Using Novel Graphene-Based Nanomaterials. *Chem. Eng. J.* 2013, *226*, 336–347. DOI: 10.1016/j.cej.2013.04.070.

[50] Dubey, S. P.; Dwivedi, A. D.; Sillanpää, M.; Lee, H.; Kwon, Y. N.; Lee, C. Adsorption of As(v) by Boehmite and Alumina of Different Morphologies Prepared Under Hydrothermal Conditions. *Chemosphere.* 2017, *169*, 99–106. DOI: 10.1016/j.chemosphere.2016.11.052.

[51] Nsiah-Gyambibi, R.; Sokama-Neuyam, Y. A.; Boakye, P.; Ampomah, W.; Aggrey, W. N.; Wang, S. Valorization of Coal Fly Ash (CFA): A Multi-Industry Review. *Int. J. Environ. Sci. Technol.* Published online April 10, 2023; *20* 11, 12807–12822. DOI:10.1007/s13762-023-04895-9.

[52] Kwiatkowski, M. Analysis of Relative Pressure Range Influence on the Identification Quality During Computer Identification of Adsorption System Parameters by Employing the New Multilayer Adsorption Models. *Appl. Surf. Sci.* 2011, *257*(21), 8912–8922. DOI: 10.1016/j.apsusc.2011.05.064.

[53] ALOthman, Z. A Review: Fundamental Aspects of Silicate Mesoporous Materials. *Materials.* 2012, *5*(12), 2874–2902. DOI: 10.3390/ma5122874.

[54] Haroon, H.; Ashfaq, T.; Gardazi, S. M. H.; Sherazi, T. A.; Ali, M.; Rashid, N.; Bilal, M. Equilibrium Kinetic and Thermodynamic Studies of Cr(vi) Adsorption Onto a Novel Adsorbent of Eucalyptus Camaldulensis Waste: Batch and Column Reactors. *Korean J. Chem. Eng.* 2016, *33*(10), 2898–2907. DOI: 10.1007/s11814-016-0160-0.

[55] Kilic, M.; Ozsin, G.; Apaydın-Varol, E.; Eren Pütün, A. Biosorption Behaviour of an Arid Land Plant, Euphorbia Rigida, Towards to Heavy Metals: Equilibrium, Kinetic and Thermodynamic Studies. *Hittite J. Sci. Eng.* 2017, *4*(2), 105–115. DOI: 10.17350/HJSE19030000056.

[56] Negarestani, M.; Mollahosseini, A.; Farimaniraad, H.; Ghiasinejad, H.; Shayesteh, H.; Kheradmand, A. Efficient Removal of Non-Steroidal Anti-Inflammatory Ibuprofen by Polypyrrole-Functionalized Magnetic Zeolite from Aqueous Solution: Kinetic, Equilibrium, and Thermodynamic Studies. *Sep. Sci. Technol.* 2023, *58*(3), 435–453. DOI: 10.1080/01496395.2022.2123743.

[57] Rajahmundry, G. K.; Garlapati, C.; Kumar, P. S.; Alwi, R. S.; Vo, D. V. N. Statistical Analysis of Adsorption Isotherm Models and Its Appropriate Selection. *Chemosphere.* 2021, *276*, 130176. DOI: 10.1016/j.chemosphere.2021.130176.

[58] Kiliç, M.; Çepelioɬullar, Ö.; Özsin, G.; Uzun, B. B.; Pütün, A. E. Evaluation of Field Debris of Chickpea Husk as a Low-Cost Biosorbent for Removal of Methylene Blue from Aqueous Solutions. *J. Faculty Eng. Architect. Gazi Univ.* 2014, *29*(4). DOI: 10.17341/gummfd.43899.

[59] Sun, H.; Zhan, J.; Chen, L.; Zhao, Y. Preparation of CTS/PAMAM/SA/Ca2+ Hydrogel and Its Adsorption Performance for Heavy Metal Ions. *Appl. Surf. Sci.* 2023, *607*, 155135. DOI: 10.1016/j.apsusc.2022.155135.

[60] Rojas, J.; Suarez, D.; Moreno, A.; Silva-Agredo, J.; Torres-Palma, T.-P. R. Kinetics, Isotherms and Thermodynamic Modeling of Liquid Phase Adsorption of Crystal Violet Dye Onto Shrimp-Waste in Its Raw, Pyrolyzed Material and Activated Charcoals. *Applied Sciences.* 2019, *9*(24), 5337. DOI: 10.3390/app9245337.

[61] Chen, X.; Hossain, M. F.; Duan, C.; Lu, J.; Tsang, Y. F.; Islam, M. S.; Zhou, Y. Isotherm Models for Adsorption of Heavy Metals from Water - a Review. *Chemosphere.* 2022, *307*, 135545. DOI: 10.1016/j.chemosphere.2022.135545.

[62] Krstić, V. Role of Zeolite Adsorbent in Water Treatment. *Handbook Of Nanomaterials For Wastewater Treatment. Elsevier*, *2021*, 417–481. DOI: 10.1016/B978-0-12-821496-1.00024-6.

[63] Hamadi, N. K.; Chen, X. D.; Farid, M. M.; Lu, M. G. Q. Adsorption Kinetics for the Removal of Chromium (VI) from Aqueous Solution by Adsorbents Derived from Used Tyres and Sawdust. *Chem. Eng. J.* 2001, *84* (2), 95–105. DOI: 10.1016/S1385-8947(01)00194-2.

[64] Febrianto, J.; Kosasih, A. N.; Sunarso, J.; Ju, Y. H.; Indraswati, N.; Ismadji, S. Equilibrium and Kinetic Studies in Adsorption of Heavy Metals Using Biosorbent: A Summary of Recent Studies. *J. Hazard. Mater.* 2009, *162*(2–3), 616–645. DOI: 10.1016/j.jhazmat.2008.06.042.

[65] Kushwaha, A.; Rani, R.; Patra, J. K. Adsorption Kinetics and Molecular Interactions of Lead [Pb(ii)] with Natural Clay and Humic Acid. *Int. J. Environ. Sci. Technol.* 2020, *17*(3), 1325–1336. DOI: 10.1007/s13762-019-02411-6.

[66] Singh, K.; Singh, A. K.; Kumar, A.; Agarwal, A. Fly Ash and TiO2 Modified Fly Ash as Adsorbing Materials for Removal of Cd(ii) and Pb(ii) from Aqueous Solutions. *J. Hazardous Materials Advances*. 2023, *10*, 100256. DOI: 10.1016/j.hazadv.2023.100256.

[67] Zhao, G. X. S.; Lee, J. L.; Chia, P. A. Unusual Adsorption Properties of Microporous Titanosilicate ETS-10 Toward Heavy Metal Lead. *Langmuir*. 2003, *19*(6), 1977–1979. DOI: 10.1021/la026490l.

[68] Basirun, A. A.; Othman, A. R.; Yasid, N. A.; Halmi, M. I. E.; Gunasekaran, B.; Shukor, M. Y. A. Adsorption Kinetics, Equilibrium, and Thermodynamic Studies to Understand Adsorption Behavior of Evans Blue Dye by Durian Husk. *Korean J. Chem. Eng.* 2023, *40*(6), 1440–1456. DOI: 10.1007/s11814-023-1434-y .

[69] Rangabhashiyam, S.; Selvaraju, N. Adsorptive Remediation of Hexavalent Chromium from Synthetic Wastewater by a Natural and ZnCl2 Activated Sterculia Guttata Shell. *J. Mol. Liq.* 2015, *207*, 39–49. DOI: 10.1016/j.molliq.2015.03.018.

[70] Wang, L.; Wang, X.; Wang, W.; Zeng, F.; Qi, L. Removal of Cr(vi) from Wastewater by M-HAFAC Based on Modified Fly Ash. *Sep. Sci. Technol.* 2023, *58* (3), 562–572. DOI: 10.1080/01496395.2022.2138435.

[71] Xiyili, H.; Çetintaş, S.; Bingöl, D. Removal of Some Heavy Metals Onto Mechanically Activated Fly Ash: Modeling Approach for Optimization, Isotherms, Kinetics and Thermodynamics. *Process Saf. Environ. Prot.* 2017, *109*, 288–300. DOI: 10.1016/j.psep.2017.04.012.

[72] Al-Harahsheh, M. S.; Al Zboon, K.; Al-Makhadmeh, L.; Hararah, M.; Mahasneh, M. Fly Ash Based Geopolymer for Heavy Metal Removal: A Case Study on Copper Removal. *J. Environ. Chem. Eng.* 2015, *3*(3), 1669–1677. DOI: 10.1016/j.jece.2015.06.005.

[73] Boycheva, S.; Zgureva, D.; Miteva, S.; Marinov, I.; Behunová, D.; Trendafilova, I.; Popova, M.; Václaviková, M. Studies on the Potential of Nonmodified and Metal Oxide-Modified Coal Fly Ash Zeolites for Adsorption of Heavy Metals and Catalytic Degradation of Organics for Waste Water Recovery. *Processes*. 2020, *8*(7), 778. DOI: 10.3390/pr8070778.

[74] Papandreou, A.; Stournaras, C. J.; Panias, D. Copper and Cadmium Adsorption on Pellets Made from Fired Coal Fly Ash. *J. Hazard. Mater.* 2007, *148*(3), 538–547. DOI: 10.1016/j.jhazmat.2007.03.020.

[75] Adamczuk, A.; Kołodyńska, D. Equilibrium, Thermodynamic and Kinetic Studies on Removal of Chromium, Copper, Zinc and Arsenic from Aqueous Solutions Onto Fly Ash Coated by Chitosan. *Chem. Eng. J.* 2015, *274*, 200–212. DOI: 10.1016/j.cej.2015.03.088.

[76] Bhattacharyya, K. G.; Gupta, S. S. Removal of Cu(ii) by Natural and Acid-Activated Clays: An Insight of Adsorption Isotherm, Kinetic and Thermodynamics. *Desalination*. 2011, *272*(1–3), 66–75. DOI: 10.1016/j.desal.2011.01.001.

[77] Arshadi, M.; Amiri, M. J.; Mousavi, S. Kinetic, Equilibrium and Thermodynamic Investigations of Ni(ii), Cd(ii), Cu(ii) and Co(ii) Adsorption on Barley Straw Ash. *Water Resour. Ind.* 2014, *6*, 1–17. DOI: 10.1016/j.wri.2014.06.001.

[78] Visa, M.; Enesca, A. Opportunities for Recycling PV Glass and Coal Fly Ash into Zeolite Materials Used for Removal of Heavy Metals (Cd, Cu, Pb) from Wastewater. *Materials*. 2022, *16*(1), 239. DOI: 10.3390/ma16010239.

[79] Huang, X.; Zhao, H.; Hu, X.; Liu, F.; Wang, L.; Zhao, X.; Gao, P.; Ji, P. Optimization of Preparation Technology for Modified Coal Fly Ash and Its Adsorption Properties for Cd2+. *J. Hazard. Mater.* 2020, *392*, 122461. DOI: 10.1016/j.jhazmat.2020.122461.